ap

Asian Journal of Physics
Vol. 26, No 2 (2017) 137-145
Available on: www.asianjournalofphysics.in

Selected recent advances in the theory and applications of photorefractive materials

Partha P Banerjee[1,2], Ujitha Abeywickrema[1] and Akash Kota[2]

[1]*Department of Electro-Optics and Photonics, University of Dayton, Dayton, OH 45469, USA*

[2]*Department of Electrical and Computer Engineering, University of Dayton, Dayton, OH 45469, USA*

Over the past fifty years, photorefractive materials have been used to various applications such as holographic data storage, non destructive testing. Propagation of electromagnetic waves inside a photorefractive material can be obtained by solving a set of coupled equations and the wave equation. The purpose of this paper is to summarize two aspects of photorefractive materials which can be used in various applications. First, the generation of higher orders inside a photorefractive material is simulated using MATLAB®. These higher orders can be used for dynamic phase shifting holography. When an optical field is applied to a photorefractive material it is deformed due to the photorefractive effect and piezoelectric effect. As the second aspect, this mechanical deformation is discussed which can be applied in the area of hybrid PR structures.

Keywords: Photorefractive materials, Nonlinearity, Two beam coupling, Diffraction orders.

1 Introduction

Photorefractive (PR) materials have been used in numerous applications over the last five decades, and the underlying theory has been developed with various approximations of the Kukhtarev equations which model the PR material [1-6]. Propagation of optical waves through a PR material demands the solutions of the coupled set of material equation and the wave equation. In this paper, we summarize two aspects of PR materials that can result in potential applications. The first pertains to propagation of beams through a PR material and simultaneous generation of higher orders, with potential applications in the area of dynamic phase shifting digital holography [7]. The second is the resulting mechanical deformation of the material due to a combination of the PR and piezoelectric effect, which can have potential applications in the area of hybrid PR structures [8].

2 The Material equations

It is well known that the following four equations, termed the Kukhtarev equations [2], model the generation of the space charge field in a PR material:

$$\frac{\partial(N_D^+ - n)}{\partial t} = -\frac{1}{q}\frac{\partial J}{\partial x} \tag{1}$$

$$\frac{\partial N_D^+}{\partial t} = (N_D - N_D^+)\,(sI + \beta) - \gamma N_D^+ n \tag{2}$$

$$J = qD\frac{\partial n}{\partial x} + q\mu n E_s + \kappa\alpha I \tag{3}$$

$$\frac{\partial D_s}{\partial x} = q(N_D^+ - N_A - n). \tag{4}$$

Corresponding author :
e-mail:pbanerjee1@udayton.edu (Partha P Banerjee)

These are, respectively, the continuity equation, the rate equation for generation of charges, the current equation, and Gauss's law, written for simplicity as a function of one (transverse dimension, . For simplicity, only scalar equations are used in the paper. In Eqs (1-4), the coupled dependent variables are:

N_D^+: ionized donor concentration;

n: electron concentration;

J: current density;

E_s: electrostatic (or space charge);

D_s: electrostatic displacement.

The constants are defined as follows

N_D: donor concentration, N_A: acceptor concentration;

γ: recombination constant;

β: thermal generation rate,

s: ionization cross-section; q: electron charge;

D: diffusion constant; μ: mobility;

κ: Photovoltaic (PV) constant; α : absorption coefficient

Also $I = |E_p|^2/2\eta$ is the intensity of the optical field E_p, which couples the above set of equations to the Helmholtz equation for optical propagation given as

$$\nabla^2 E_p + k^2 E_p = 0 \tag{5}$$

where k is the propagation constant in the medium and η is the characteristic impedance of the medium. Now k^2 can be expressed as

$$k^2 = n^2 k_0^2 = (n_0 + \Delta n)^2 k_0^2 \approx n_0^2 k_0^2 + 2 n_0 \Delta n k_0^2 \tag{6}$$

where n_0 is the refractive index of the material, k_0 is the propagation constant in free space and $\Delta n << n_0$ is the induced refractive index which is related to the elctrostatic field E_s through the electrooptic coefficient r of the material through the relation

$$\Delta n \approx -\frac{1}{2} n_0^{\ 3} r E_s \tag{7}$$

Clearly the five dependent variables for the Kukhtarev equations listed above cannot be solved with the four available Eqs (1-4). The missing equation is the constitutive relation for the electrostatic field. In the simplest case, $D_s = \epsilon E_s$, where ϵ is the permittivity; however, more generally [5,9-11],

$$D_s = eS + \epsilon E_s \tag{8}$$

$$T = cS - eE_s + p' I \, , \, p' = \frac{\epsilon_0 \eta n_0^4}{2} p \tag{9}$$

where the newly introduced dependent variables are the strain S and strain T, and where the new constants are

e: piezoelectric constant, c: elastic constant; p: elasto-optic constant; ϵ_0; free space permittivity

Finally the stress S and strain T are related through the elastodynamic equation

$$\rho \frac{\partial^2 U}{\partial t^2} = \frac{\partial T}{\partial z} \, , \, S = \frac{\partial U}{\partial z} \tag{10}$$

where U is the particle displacement, and where ρ denotes the density. In Eq. (10), only the components of stress and strain in the nominal direction of propagation of the optical field is considered.

In general, the set of equations (1)-(4) and (8-10) involving 7 dependent variables describing the *complete* set of material equations need to be solved along with the Helmholtz equation for the optical field,

since the material equations and the Helmholtz equation are coupled through the presence of the intensity term I.

The Kukhtarev equations in *steady state* ($\frac{\partial}{\partial t} = 0$) can be simplified as follows. First for the purely diffusive case, i.e., from Eq. (1), $J = 0$, substituting this in Eq (3) results in

$$E_s = \frac{k_B T}{q} \frac{1}{n} \frac{\partial n}{\partial x} \tag{11}$$

where the relation $\frac{D}{\mu} = \frac{k_B T}{q}$ has been used. Now, from Eq (2),

$$N_D^+ = \frac{N_D}{1 + \frac{\gamma n}{sI + \beta}} \tag{12}$$

Also, from Eq (4),

$$N_D^+ = \frac{1}{q} \frac{\partial D}{\partial x} + N_A \tag{13}$$

assuming $n << N_D^+ - N_A$ .Equating Eqs (12) and (13),

$$n = \frac{sI + \beta}{\gamma} \left[\frac{N_D}{N_A + \frac{1}{q} \frac{\partial D}{\partial x}} - 1 \right] \tag{14}$$

Now taking $\frac{1}{q} \frac{\partial D}{\partial x} << N_A$,

$$n \approx \frac{sI + \beta}{\gamma} \frac{N_D}{N_A} \tag{15}$$

where a further assumption, viz., $N_D >> N_A$ has been employed. Finally, substituting Eq (16) in Eq (11), the induced electrostatic field in the PR material can be expressed as [12]

$$E_s \approx - \frac{k_B T}{q} \frac{\partial I / \partial x}{I + \beta / s} \tag{16}$$

Equation (16) describes the dependence of the induced electrostatic field on the intensity in a PR material where the dominant charge transport mechanism is diffusion dominated. The quantity β/s is referred to as the dark current I_d. Now, for a sinusoidal intensity distribution, such as that formed from the intereference of two plane waves traveling at an angle and incident on a PR medium,

$$I + \beta/s = I + I_d = I_0 + I_1 \cos Kx + I_d \tag{17}$$

If now $I_0 + I_d >> I_1 \cos Kx$, then from Eq (16), it is clear that $E_s \propto \nabla I$ for a diffusion dominated PR material.

In a PR material where the PV contribution dominates, the Kukhtarev equations can be approximately simplified to [12]

$$E_s \approx - \frac{\kappa \alpha \gamma}{\mu q s} \frac{N_D}{N_A} \frac{I}{I + \beta/s} \approx \frac{\kappa \alpha \gamma}{\mu q \beta} \frac{N_D}{N_A} I \tag{18}$$

where the condition $I << \beta/s$ has been imposed.

As mentioned above, a PR material may also exhibit piezoelectric and photoelastic properties. The effect of this on the induced refractive index has been extensively studied. In this paper, a simple example of the induced strain giving rise to surface corrugation for an unclamped (or free) PR material is described. Assuming steady state, Eq (10) gives $\frac{\partial T}{\partial z} = 0$ or

$$T = T_0 = const. \tag{19}$$

Substituting this in Eq (9),

$$T = c\frac{\partial U}{\partial x} - eE_s + P'I. \tag{20}$$

Then for a diffusion dominated PR material, using Eqs (16) and (20),

$$U = \frac{1}{c}\int\left[T_0 + P'I - e\frac{k_BT}{q}\frac{\partial I/\partial x}{I+\beta/s}\right]dz \tag{21}$$

Assuming again that $I = I_0 + I_1 \cos kx$ and setting $T_0 = -P'I_0$, Eq (21) yields

$$U = \frac{p'I_1L}{c}\cos Kx + \frac{e}{c}\frac{k_BTKL}{q}\frac{sinKx}{I_0+\beta/s}, \tag{22}$$

which is the particle displacement in a diffusion dominated PR material for a PR material of thickness L.

Similarly, for a PV dominated unclamped PR material, the particle displacement, using Eqs (18) and (20), is given by [11,13]

$$U = \frac{(p' + e\frac{\kappa\alpha\gamma}{\mu q\beta}\frac{N_A}{N_D})I_1L}{c}cosKx \tag{23}$$

where the same kind of (cosinusoidal) intensity distribution as above has been assumed.

In the following Sections, two illustrative cases using the derivations above are considered. The first example demonstrates *beam* coupling in a PV dominated PR material such as $LiNbO_3$ leading to the generation of higher (non-Bragg) orders. The second example pertains to theoretical predictions and experimental evidence of induced surface corrugation during the writing of gratings in PR $LiNbO_3$.

3 Bragg and Non-Bragg Orders during Two Beam Coupling in PR $LiNbO_3$

In this Section, the propagation of two beams traveling at an angle and intersecting in a PR material such as $LiNbO_3$ is analyzed numerically. The intensity grating I gives rise to a refractive index grating Δn which couples not only the two incident beams but is also responsible in the creation of higher non-Bragg orders due to the finite thickness of the grating. Using Eqs (7) and (18), the induced refractive index can be expressed as

$$\Delta n = CI,\ C \approx -\frac{1}{2}n_o^3 r\frac{\kappa\alpha\gamma_R N_A}{\mu q N_D\beta} \tag{24}$$

Using $\frac{N_A}{N_D} = \frac{1}{2}$, $\gamma_R = 10^{-15}$ m^3/s, $k = 3\cdot10^{-11}$A · m/W, α = 130 m^{-1}, $\mu = 10^{-6}$ m^2/V. s, $\beta = 1$s^{-1}, $q = 1.6\cdot10^{-19}$ C, $r = 30.8$ pm/V, $n_0 = 2.22$, $s = 6\cdot10^{-5}$m^2/J, the value of the constant C is $C = -2.1\cdot10^{-11}$ m^2/W. All the material parameters used in the calculation of photovoltaic coefficient are taken from Ref. [12].

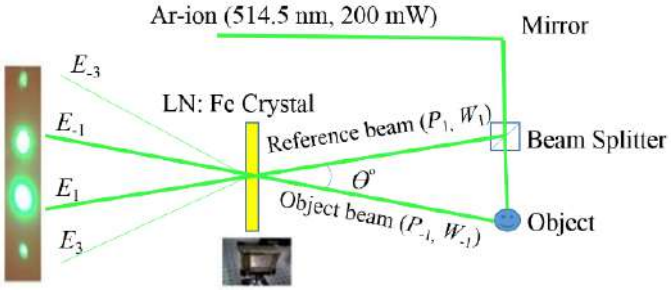

Fig 1. Experimental set up for recording hologram in LN. The Bragg (E_1,E_{-1}) and non-Bragg (E_3,E_{-3}) orders are shown to the left of the figure [14].

The amplitudes and phases for the Bragg and non-Bragg orders can be found by first decomposing the total optical field inside PR $LiNbO_3$ as [14,15]

$$E_p(x,z) = (E_1(z)e^{-j(k/2)x} + E_{-1}(z)e^{+j(k/2)x} + E_3(z)e^{-j3(k/2)x} + E_{-3}(z)e^{+j3(k/2)x})\, e^{-jk0z} \tag{25}$$

where x denotes the transverse direction and z denotes the nominal direction of propagation.

E_l, $l = 1, -1, 3, -3$ denotes the optical field for l^{th} order and

$$K = 2k_0 \sin(\theta/2), \tag{26}$$

where K is the spatial frequency of Bragg grating, k_0 is the propagation constant in free space, and θ is the angle between the incident beams. Substituting Eq. (25) in to the Helmholtz equation Eq. (5), and using Eq. (6) along with Eq (24), the spatial evolution equations for the two Bragg (E_1, E_{-1}) and first two non-Bragg (E_3, E_{-3}) orders can be determined, after some algebra, as [15]:

$$\frac{\partial E_1}{\partial z} = -jk_0E_1\left[c(|E_1|^2 + 2|E_{-1}|^2 + 2|E_3|^2 + 2|E_{-3}|^2) - \frac{1}{2}\left(\frac{K}{2k_0}\right)^2\right]$$
$$-jk_0c\,[2E_3E_{-1}E_1^* + 2E_3E_{-3}E_{-1}^* + 2E_{-1}E_{-1}E_{-3}^*], \tag{27a}$$

$$\frac{\partial E_{-1}}{\partial z} = -jk_0E_{-1}\left[c(2|E_1|^2 + |E_{-1}|^2 + 2|E_3|^2 + 2|E_{-3}|^2) - \frac{1}{2}\left(\frac{K}{2k_0}\right)^2\right]$$
$$-jk_0c\,[2E_{-3}E_1E_{-1}^* + 2E_3E_{-3}E_1^* + 2E_1E_1E_3^*], \tag{27b}$$

$$\frac{\partial E_3}{\partial z} = -jk_0E_3\left[c(2|E_1|^2 + 2|E_{-1}|^2 + |E_3|^2 + 2|E_{-3}|^2) - \frac{9}{2}\left(\frac{K}{2k_0}\right)^2\right]$$
$$-jk_0c\,[2E_1E_{-1}E_{-3}^* + 2E_1E_1E_{-1}^*], \tag{27c}$$

$$\frac{\partial E_{-3}}{\partial z} = -jk_0E_{-3}\left[c(2|E_1|^2 + 2|E_{-1}|^2 + 2|E_3|^2 + |E_{-3}|^2) - \frac{9}{2}\left(\frac{K}{2k_0}\right)^2\right]$$
$$-jk_0c\,[2E_1E_{-1}E_3^* + 2E_{-1}E_{-1}E_1^*]. \tag{27d}$$

Since our objective is to study interaction between beams, we decompose every order into its angular plane wave spectrum. Therefore, each order, viz., E_n , is written as a collection of plane waves as [15]

$$E_n = \sum_{i=-\infty}^{\infty} E'_{ni}\, e^{-ji\Delta Kx} \tag{28}$$

where E'_{ni} denotes the amplitude of the i^{th} angular component of E_n , ΔK is the magnitude of the fundamental spatial frequency component in the angular plane wave spectrum profile. By replacing each diffracted order with its corresponding spectrum, the coupled interaction equations of the spectra of the various orders are obtained. These equations are algebraically complicated, we write one of the equations for the i-th spectral amplitude of the +3 non-Bragg order as an example [15]:

$$\left(\frac{\partial E'_{3i}}{\partial z}\right) = -jk_0c_1\,[2\Sigma_\beta\Sigma_\alpha E'_{1\alpha}E'^{*}_{1(\beta-\alpha)}E'^{*}_{3(i-\beta)} + 2\Sigma_\beta\Sigma_\alpha E'_{-1\alpha}E'^{*}_{-1(\beta-\alpha)}E'_{3(i-\beta)} + \Sigma_\beta\Sigma_\alpha E'_{3\alpha}E'^{*}_{3(\beta-\alpha)}E'_{3(i-\beta)}$$
$$+ 2\Sigma_\beta\Sigma_\alpha E'_{-3\alpha}E'^{*}_{-3(\beta-\alpha)}E'_{3(i-\beta)} + 2\Sigma_\beta\Sigma_\alpha E'_{-1\alpha}E'_{1(\beta-\alpha)}E'^{*}_{-3(i-\beta)} + \Sigma_\beta\Sigma_\alpha E'_{1\alpha}E'_{1(\beta-\alpha)}E'^{*}_{-1(i-\beta)}$$
$$-jk_0\frac{9}{2}\left(\frac{ik+K}{2k_0}\right)^2 E'_{3i}. \tag{29}$$

Figure 2(a, b) illustrate the spatial evolutions of the non-Bragg orders in PR LN for the casewhere $P_1 = 20$ mW, $P_{-1} = 2$ mW; $W_1 = W_{-1} = 0.4$ mm; $\theta = 0.5°$. As expected, there is no energy coupling between the Bragg orders due to the nature of the induced nonlinearity, which gives rise to purely phase coupling. The difference between the peak intensities of E_3 and E_{-3} are in agreement with the fact that from Eqs. (27c,d) it is evident that the dominant terms responsible for the evolution of non-Bragg orders E_3 and E_{-3} are $E_1\, E_1\, E_{-1}^*$ and $E_{-1}\, E_{-1}\, E_1^*$, respectively. Note that there appears to be mode conversion of the incident Gaussian beams in the higher orders due to interaction of the Gaussian beams in the PR material. As the angle between the incident Gaussian beams increases, there is periodic mode conversion for these non-Bragg orders in the PR material. Details of this periodic mode conversion and its dependence on interaction angle and the widths of the incident Gaussian beams is described in detail in Refs. [15,16].

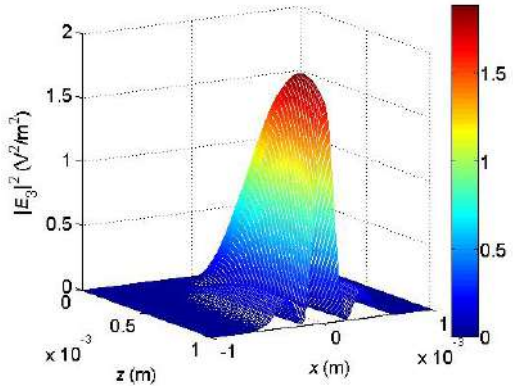

(a)

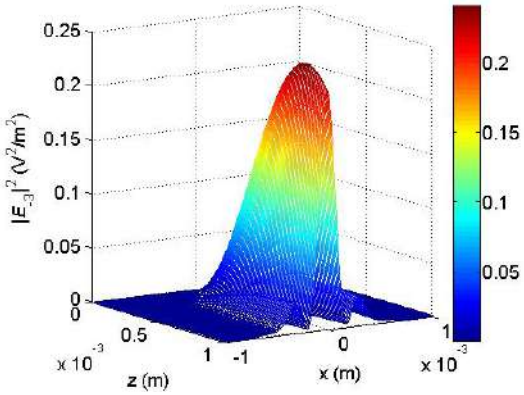

(b)

Fig 2. Spatial evolution of (a) first non-Bragg order (E_3), and (b) second non-Bragg order (E_{-3}) in PR $LiNbO_3$. $P_1 = 20\ mW$, $W_1 = 0.4\ mm$; $P_{-1} = 2mW$, $W_{-1} = 0.4\ mm$ [15].

4 Surface Corrugation during Two Beam Coupling in PR $LiNbO_3$

In Section 2, the surface corrugation induced in PR $LiNbO_3$ has been derived. Using the material parameters in Section 3, along with $\kappa = 3 \times 10^{-11} A \cdot \frac{m}{W}$, $\alpha = 130 m^{-2}$, $e = 30 \text{C/m}^2$, $c = 2 \times 10^{-11}\ \text{N/}m^2$, $P = 0.1$,

an approximate estimate for the peak displacement for $I_1 \approx 10^3$ W/m^2 is of the order of a few *nm*. To observe this by experiment, a virgin sample of 50 × 50 × 2 mm^3 PR $LiNbO_3$:Fe is used to record gratings using a 514 nm Ar-ion laser source. The angle between the beams is approximately 1 degree, corresponding to a grating period of about 30 microns. After the grating is written, it is mounted on a motorized rotational stage and then read by a 633 nm He- Ne laser, as shown in Fig 3(a). The diffracted and undiffracted order intensities are measured as a function of the incident angle. Since Fabry-Perot effects may contribute to the variation of the intensity as a function of the incident angle, the observed intensity variations are re-plotted as a function of the square of the incident angle (since $sin\theta \approx \theta$), Fourier transformed and numerically filtered to remove the Fabry-Perot effect. Details are provided in Ref. [13]. Subsequently, the intensity variations are plotted as a function of the incident angle, a typical plot is shown in Fig 3(b). The period is $2\phi_B = 1.2°$, where ϕ_B is the Bragg angle consistent with the 633 nm reading light. The diffraction efficiency can be calculated by monitoring the peak to peak variations of the power in the +1 and 0^{th} orders. Now, using the relationship for the diffraction efficiency for the 1st order for a surface relief grating given by [17]

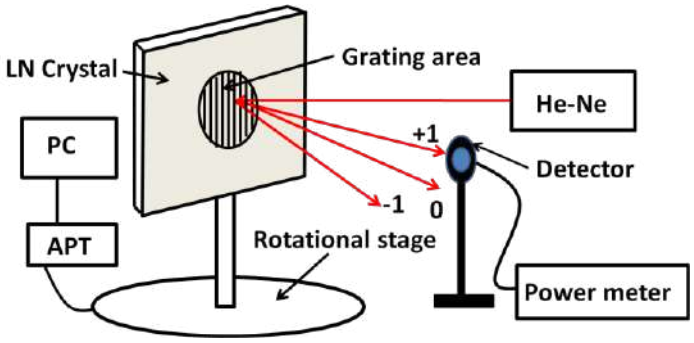

(a)

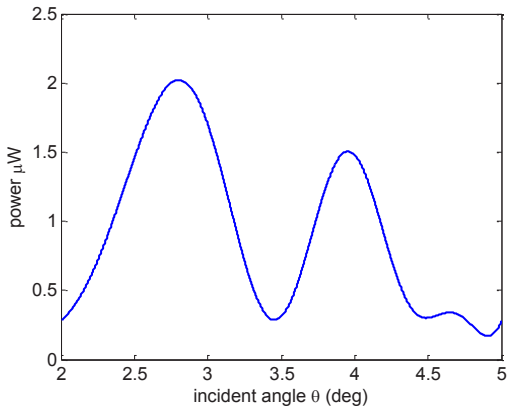

(b)

Fig 3 (a). Experimental setup for recording intensities of diffraction orders as a function of the incident angle θ_i . Grating area is illuminated with a He-Ne laser (633 nm) and the power of the each order is measured using a power meter. Rotational stage with a stepper motor is used and controlled by connected to a computer through the APT^{TM} stepper motor controller. Rotational stage is rotated increments of 0.1 degrees; (b) Variation of intensity of the +1 order as a function of incident angle, with the Fabry-Perot effect eliminated through signal processing [13].

$$\eta = \left[\frac{2}{\pi}\sin\left(\frac{k_0(n_0-1)U_0}{2}\right)\right]^2, \tag{30}$$

the experimentally inferred estimate for the peak displacement is approximately 20 *nm*, in qualitative agreement with theoretically predicted results. This is also in agreement with the findings of Sarkisov *et al* [10].

5 Conclusion

Although the PR effect has been discovered over 40 years ago and enormous amount of work has been done regarding its theory and applications, new niche areas for potential applications continue to be discovered. In this paper, we have reviewed two of the recent developments which we have been engaged in recently. Higher order generation has potential applications in phase-shifting digital holography. Surface corrugations have potential applications in hybrid PR devices with sandwiched liquid crystals which can vastly improve the two-beam coupling strength in such devices. Although a very simplistic scalar version of the material, constitutive and wave equations have been discussed in this paper, a rigorous analysis is necessary for accurate calculations. It is hoped that novel applications of PR materials continue to evolve in the future.

6 References

1. Kukhtarev N, Kinetics of recording and erasing of holograms in electro-optical crystal, *Sov Tech Phys Lett*, 2(1976)438-442.
2. Yeh P, *Introduction to Photorefractive Nonlinear Optics* (Wiley, New York), 1993.
3. Gunter P, Huignard J P (eds), *Photorefractive Materials and their Applications* 1-3 (Springer, Berlin, 2006, 2007, 2007).
4. Yu FTS, Yin S (eds), *Photorefractive Optics: Materials, Properties and Applications,* (Academic Press, New York), 1999.
5. Solymar L, Webb D J, Grunnet-Jepsen A (eds), *The Physics and Applications of Photorefractive Materials* ,(Clarendon Press, Oxford), 1996.
6. Blanche P A (ed), *Photorefractive Organic Materials and Applications* (Springer, Berlin), 2016.
7. Nehmetallah G, Banerjee P P, Applications of digital and analog holography in three-dimensional imaging, *Adv Opt Photon*, 4(2012)472-553.
8. Reshetnyak V Y, Pinkevych I P, Sluckin T J, Cook G, Evans D R, Beam coupling in hybrid photorefractive inorganic-liquid crystal liquid crystal cells – impact of optical rotation, *J Appl Phys*, 115(2014)103103; doi: 10.1063/1.4867479
9. Litvinov R, Shandarov S, Influence of piezoelectric and photoelastic effects on pulse hologram recording in photorefractive crystals, *J Opt Soc Am B*, 11(1994)1204-1210.
10. Sarkisov S, Curley M, Kukhtarev N, Fields A, Adamovsky G, Smith C, Moore L, Holographic surface gratings in iron-doped lithium niobate, *Appl Phys Lett*, **79**(2001)901- 903.
11. Shandarov S, Shmakov S, Zuev P, Burimov N, Kargin Yu, Shepelevich V, Ropot P, Gudelev V, Contribution of the inverse flexoelectric effect to counterpropagating two-wave mixing of light beams in photorefractive crystals, *J Opt Tech*, 80(2013)409-414.
12. Liu J-J, Banerjee P, Song Q, Role of diffusive, photovoltaic, and thermal effects in beam fanning in $LiNbO_3$, *J Opt Soc Am B*, 11(1994)1688-1693.
13. Abeywickrema U, Banerjee P, Evans D, Holographic surface gratings in photorefractive materials, *Proc OSA* FW4A.3, 1–2 (2015).
14. Kota A, Abeywickrema U, Banerjee P, Spectral analysis of Bragg and non-Bragg orders in dynamic holography using photorefractive materials, *Proc OSA* JW4A.86, 1-2 (2016).
15. Kota A, Abeywickrema U, Banerjee P, Interaction of angular plane wave spectra of Bragg and non- Bragg orders in photorefractive lithium niobate," *Proc SPIE*, **9959** 99590C-1-7 (2016).

16. Kota A, Spectral analysis of Bragg and non-Bragg orders in dynamic holography using photorefractive materials, MS Thesis, University of Dayton, (2016).
17. de Jong T M, de Boer D K G, Bastiaansen C W M, Surface-relief and polarization gratings for solar concentrators, *Opt Express*, 19(2011)15127-15142.

[*Received*: 19.2.2017; *accepted*: 28.2.2017]

Dr. Partha Banerjee is a Professor and the Chair of the Department of Electro-Optics and Photonics and a Professor of Electrical and Computer Engineering with the University of Dayton, Dayton, OH,USA, where he was the Chair of the Department of Electrical and Computer Engineering from 2000 to 2005. Prior to that, he was with the University of Alabama in Huntsville, Huntsville, AL, USA, from1991 to 2000, and Syracuse University, Syracuse, NY, USA, from 1984 to 1991. He received the M.S. and Ph.D. degrees from the University of Iowa, Iowa City, IA, USA, in 1980 and 1983, respectively. His areas of research interest are digital holography, metamaterials, nonlinear optics, photorefractives, and acoustooptics. He has authored and co-authored five textbooks, 10 book chapters, over 120 refereed journal articles, and over 150 conference papers/presentations. He was the General Co-Chair of OSA's Digital Holography topical meeting in 2010, and is a Topical Editor of Applied Optics. He is a fellow of OSA, SPIE, and IoP. He was a recipient of the NSF Presidential Young Investigator Award in 1987

Ujitha Abeywickrema received his BS degree in Physics from University of Colombo, Sri Lanka in 2007, his MS degree in Physics from the University of Akron in 2011, and his PhD degree in Electro-Optics from University of Dayton in 2015. Currently, he is a research scientist at the department of Electro-Optics and Photonics, University of Dayton. His research interests are holographic topography and tomography, dynamic holography using photorefractive materials, and bulk crystal growing.

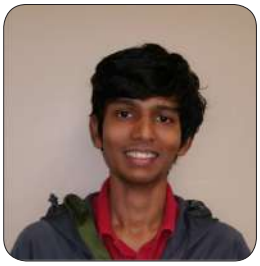

Akash Kota received his B.Tech degree in Electrical Engineering from K L University in 2013 and his MS degree in Electrical Engineering from University of Dayton in 2016. Currently he is a PhD student in Electrical Engineering at the University of Dayton. His research interests are digital holography, photorefractive materials, and Bio-MEMS. His PhD work includes study of ion-channel currents in human cardiac cells using MEMS based silicon structure.